ISSN: 2688-8645

Preparation and Release Mechanism of Natural-Skeleton Sustained-Release Tracer Particles

Yufei Liu

School of Xi'an Petroleum University, Xi'an, Shaanxi, 710065, China

Abstract

In the current field of petroleum development, water-source identification and water shutoff in horizontal wells have become key difficulties affecting the sustained development of such wells. Intelligent tracer-based water diagnosis and shutoff technology can provide highly intuitive information on the location and intensity of water production along the horizontal section and therefore has broad development prospects. However, the long-term performance of intelligent tracer-based water shutoff in horizontal wells is influenced by many factors, such as erosion by formation fluids and aging of shutoff materials. In field applications, effective methods for monitoring and evaluating the long-term effect of water shutoff treatments are still lacking, making it difficult to accurately judge their long-term effectiveness. A better understanding of the dominant factors controlling the sustained-release behavior of intelligent tracers, and further optimization of that behavior, is a prerequisite for subsequent intelligent tracer-based water-control operations in horizontal wells. Therefore, taking a self-developed water-soluble intelligent tracer as the research object, this paper investigates its macroscopic physical properties and microstructure by CT scanning. Based on the characteristics of its physical skeleton, a suitable sustained-release tracer was selected, and static scouring experiments were carried out. The sustained-release behavior was qualitatively analyzed from four aspects: scouring flow rate, temperature, particle diameter, and active-component content. The static scouring experiments demonstrate that this natural skeleton can realize rapid tracer release and satisfy the requirement of sensitivity to water-flow velocity. The experiments also show that scouring flow rate and temperature are the main factors affecting sustained-release performance; within an appropriate range, higher temperature and higher scouring flow rate accelerate the release process. Particle diameter and active-component content are not the dominant control factors. Among the four factors, scouring flow rate has the strongest effect. Under a certain scouring rate, the tracer component stored inside the skeleton can be released rapidly, and the release efficiency can approach 100%. The results indicate that this intelligent tracer can be released rapidly in the short term and is highly sensitive to water-flow velocity. It can provide a rapid evaluation tool for subsequent field water-finding and water-shutoff operations, and it also provides a reference for selecting skeleton materials and tracer components for sustained-release tracer particles and for interpreting tracer-concentration curves.

Keywords

Natural Skeleton; Release Mechanism; Experimental Preparation; Sustained-release Tracer; Intelligent Tracer.

1. Introduction

At present, most oilfields in China have entered the tertiary recovery stage. Waterflooding is the main development mode for domestic oil and gas fields, and the associated problems of water breakthrough and flooding are becoming increasingly prominent. The water cut of

ISSN: 2688-8645

produced fluids continues to rise, and the productivity of individual wells declines rapidly, especially in reservoirs with active edge water or bottom water [1]. Traditional investigation methods are not only operationally complex, cumbersome, and expensive, but are also prone to sticking and obstruction and may affect the normal production of oil wells. During zonal testing, other intervals must be shut in, so the measured results cannot reflect the actual conditions of a horizontal well under normal production [2]. Therefore, in order to obtain accurate information on water-entry position, breakthrough time, and flow parameters, to enhance the effectiveness of profile control and water shutoff, and to significantly improve recovery, oilfield tracer technology has emerged.

In recent years, tracer research and development technology in China has undergone multiple rounds of iteration and improvement. It was initially developed and applied in oilfields such as Dagang and Shengli in the early 1980s [3]. Chemical tracers, as the first generation of oilfield tracers, initiated the application of tracer technology in oilfield development [4]. Subsequently, radioactive-isotope tracers and trace-substance tracers, representing the second, third, and fourth generations of oilfield tracers, were also promoted and applied [5-10]. However, each of these tracers has its own limitations. Modern oilfield tracers require higher levels of intelligence and autonomy, which has driven the rapid development and field application of intelligent tracer technology [11-13]. It has now been applied in several domestic and overseas oilfields.

According to their dissolution media, intelligent tracers can be divided into two categories: water-soluble tracers and oil-soluble tracers. They are mainly composed of a skeleton and a tracer component [11-13]. When an intelligent tracer is used, it is installed in advance in a production short joint and then run into the wellbore. Different tracer-containing short joints can be placed at different positions along the production section of a horizontal well. Once fluid flows through the interval, the solid tracer dissolves into the corresponding water or oil phase. The produced concentration of tracers from different short joints is then sampled and detected at the wellhead, and subsequent data interpretation can be used to determine the specific water-entry position and other production parameters. In practice, tracer release is a complex dynamic process jointly controlled by the skeleton itself and the external environment, such as temperature and external fluid scouring velocity. Its release rate changes continuously. If the cumulative contribution of water produced from different intervals along the horizontal section is not considered, large differences among water-producing intervals during the middle and late monitoring stages may lead to misidentification of the main water-producing layer.

Therefore, taking a self-developed water-soluble intelligent tracer as the research object, this study investigates its macroscopic physical properties and microstructure through CT scanning, selects a suitable sustained-release tracer based on the characteristics of the physical skeleton, and carries out static scouring experiments. The sustained-release behavior is qualitatively analyzed from four aspects: scouring flow rate, temperature, particle diameter, and active-component content. The results show that this natural skeleton can realize rapid tracer release and meet the requirement of sensitivity to water-flow velocity. Scouring flow rate and temperature are the main factors affecting the release behavior, whereas particle diameter and active-component content are secondary factors. Scouring flow rate has the strongest effect, and under certain conditions the release efficiency can approach 100%. Combined with the physical-property analysis of the intelligent-tracer skeleton and tracer component and the dynamic simulation experiments on influencing factors, the study demonstrates that this intelligent tracer is highly sensitive to water-flow velocity and can be released rapidly within a short time. The results can accelerate the development of short-term intelligent tracer water-shutoff materials in China, provide a rapid evaluation tool for subsequent field water-finding and water-shutoff operations, and offer a reference for selecting skeleton materials and tracer components for sustained-release tracer particles and interpreting tracer concentration curves.

ISSN: 2688-8645

2. Preparation of Natural-Skeleton Sustained-Release Tracer Particles

2.1. Selection of the Natural Skeleton

For the selection of the natural skeleton, several candidate materials were considered, including vermiculite, expandable clay, and perlite. During drying, vermiculite tends to expand markedly in volume, whereas expandable clay readily disintegrates during solution adsorption. Perlite is an acidic lava formed after volcanic eruptions, and its main component is silica. Because of differences in water content, perlite expands after high-temperature heating to form lightweight and porous particles. After crushing and heating, the internal water in perlite evaporates rapidly, causing the raw material to expand to 4-20 times its original volume and to form a foamed structure. This process gives perlite particles the characteristics of low density and high porosity. Perlite also exhibits good heat resistance and chemical stability.

As shown by the CT image of perlite (Fig. 1), the perlite matrix contains a large number of pore channels that can serve as storage sites for the tracer, and the good connectivity of these channels facilitates rapid release. Therefore, the material is expected to be highly sensitive to water-flow velocity.

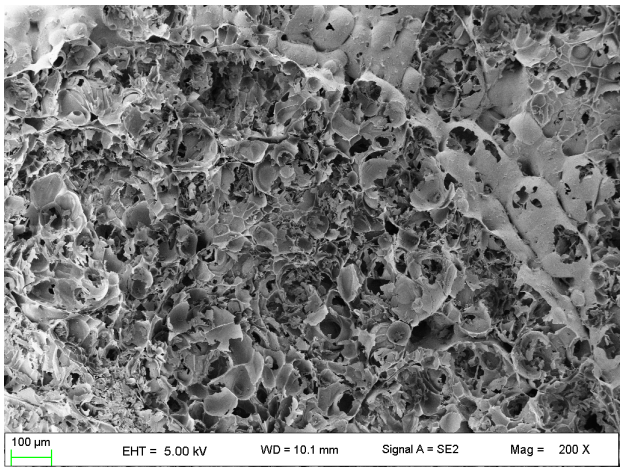

Fig 1. CT image of the perlite matrix

Because this study needed to control particle size and evaluate the effect of different particle sizes on sustained release, three perlite particle-size ranges were selected: 2-4 mm, 3-6 mm, and 4-8 mm.

Table 1. General chemical composition of perlite (wt.%)

Component	Content
SiO_2	68-74
Al_2O_3	±12
Fe_2O_3	0.5-3.6
CaO	0.7-1.0
Na_2O	2-3
K_2O	4-5
TiO_2	0.3
H_2O	2.3-6.4

ISSN: 2688-8645

2.2. Selection of the Active Tracer Component

In selecting the tracer component, considerations included economic affordability, experimental safety and controllability, and environmental friendliness. Sodium bromide is a common inorganic compound that usually appears as white crystals or granules. Under normal conditions, its melting point and boiling point can reach 755°C and 1390°C, respectively. Sodium bromide has high solubility in water and releases a certain amount of heat during dissolution. The bromide ion is chemically stable and not prone to reaction. In addition, the background adsorption of sodium bromide is relatively low, which favors accurate detection. Therefore, sodium bromide was finally selected as the active tracer component of the natural-skeleton material.

2.2.1. Determination of the Maximum Absorption Wavelength of Bromide Ion

The tracer used in this study was sodium bromide. For performance evaluation, the concentration of bromide ions in solution first had to be measured by ultraviolet spectrophotometry. To ensure experimental accuracy, the maximum absorption wavelength of bromide ion was determined first, and then a standard concentration curve for sodium bromide solution was established. The experiments showed that the maximum absorption wavelength of bromide ion was 207 nm. Therefore, 207 nm was selected for subsequent absorbance measurements to ensure the accuracy of the experimental data.

2.2.2. Establishment of the Standard Curve for Sodium Bromide Solution

Based on the above result, the maximum absorption wavelength of bromide ion in sodium bromide solution was set at 207 nm. A stock solution of sodium bromide with a concentration of 100 mg/L was prepared, and 0.5, 1.0, 2.5, 4.0, 5.0, 10.0, 20.0, and 30.0 mL aliquots were accurately pipetted into 50 mL volumetric flasks. After dilution with distilled water, sodium bromide solutions with concentration gradients of 1, 2, 5, 8, 10, 20, 40, and 60 mg/L were obtained for later measurement.

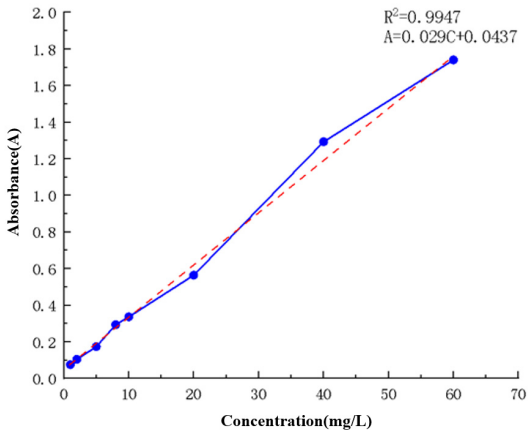

Fig 2. Standard curve for bromide ion concentration and absorbance

The absorbance values of the solutions were then measured using a spectrophotometer. By linearly fitting the experimental data obtained for sodium bromide solutions with different concentrations, the standard-curve equation for bromide ion in sodium bromide solution was determined as A = 0.029C + 0.0437, with R^2 = 0.9947. The fitted curve is shown in Fig. 2. The experimental curve shows good agreement with the standard curve and can therefore be used as the calculation curve for this study.

ISSN: 2688-8645

After sampling in the subsequent experiments, the absorbance of bromide ions measured for each test group can be converted into the corresponding concentration using the standard curve, thereby providing the basis for subsequent data processing.

2.3. Laboratory Preparation of Natural-Skeleton Sustained-Release Tracer Particles

2.3.1. Experimental Equipment

1) 101-0AB electric blast drying oven.

2) One 10 mL graduated cylinder, several 500 mL beakers, several metal trays, and one glass rod.

3) One each of 1, 2, 5, and 10 mL pipettes.

4) TP-A2000 electronic balance (accuracy: 0.1 g; range: 10 kg).

2.3.2. Preparation Procedure

(1) Weighing of perlite: using an electronic balance, seven 50 g batches of 2-4 mm perlite particles, one 50 g batch of 3-6 mm particles, and one 50 g batch of 4-8 mm particles were weighed and placed into nine identical beakers for later use.

(2) Preparation of sodium bromide solutions with different mass fractions: 50, 100, and 150 g of sodium bromide granules were weighed, and 450, 400, and 350 mL of purified water were placed into three separate 500 mL beakers. The sodium bromide granules were then added to the corresponding beakers and stirred with a glass rod until fully dissolved. If necessary, gentle heating without evaporating water was applied. After complete dissolution, sodium bromide solutions with mass fractions of 10%, 20%, and 30% were obtained for later use.

(3) Adsorption of the reagent: the particles to be impregnated were placed into a clean 500 mL beaker, and a 10% sodium bromide solution was added until the solution level was 1-2 cm above the particles. The particles were then left to stand for 10 min, after which adsorption was considered complete. The same procedure was followed for the other eight groups. To satisfy the controlled-variable design of this study, seven groups of perlite particles adsorbing a 10% sodium bromide solution, one group adsorbing a 20% solution, and one group adsorbing a 30% solution were required. If the prepared sodium bromide solution was insufficient, additional solution was prepared according to step (2).

(4) Drying of the particles: the nine groups of impregnated particles were first preliminarily filtered on wire mesh and placed on metal trays. They were then dried in a 90°C oven. The mass of each group was measured every hour during drying. When the mass change within 1 h was less than 1 g, the drying process was terminated. After drying, the mass of each group of perlite particles was weighed again, and the mass of adsorbed reagent was calculated. The dried particles were then stored in a sealed condition to prevent moisture uptake from the air before the subsequent experiments.

2.3.3. Preparation Results

By following the above procedure, nine groups of perlite particles were prepared as listed in Table 2.

3. Release Mechanism of Natural-Skeleton Sustained-Release Tracer Particles

This section first determines the experimental program for performance evaluation so as to prepare adequately for investigating the performance of natural-skeleton sustained-release tracer particles. Four factors are considered: scouring flow rate, temperature, particle diameter, and active-component content. The purpose is to evaluate the performance of the skeleton-type

ISSN: 2688-8645

sustained-release tracer particles and to identify the laws governing the effect of these factors on sustained-release behavior.

Table 2. Prepared perlite-particle samples

No.	Mass before adsorption (g)	Mass after adsorption (g)	Particle size (mm)
1	50	80.0	2-4
2	50	76.7	3-6
3	50	72.3	4-8
4	50	80.0	2-4
5	50	80.0	2-4
6	50	80.0	2-4
7	50	110.2	2-4
8	50	120.4	2-4
9	50	80.0	2-4

3.1. Experimental Equipment and Setup

1) 754 UV-Vis spectrophotometer.

2) HH-1A electric thermostatic water bath.

3) KY-300EL-I/MN2 peristaltic pump.

4) 250 mL and 500 mL beakers, 250 mL graduated cylinders, 100 mL and 50 mL volumetric flasks, 2 mL pipettes, pipette bulb, etc.

The schematic diagram and photograph of the experimental apparatus are shown in Figs. 3 and 4.

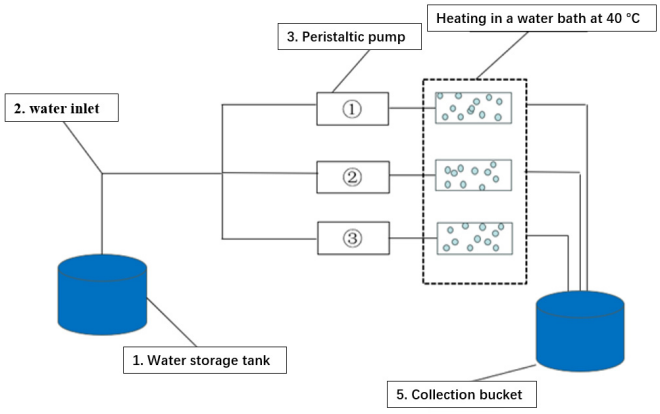

Fig 3. Schematic diagram of the experimental setup

3.2. Experimental Program

3.2.1. Effect of Scouring Flow Rate on Sustained-Release Performance

(1) Prepare several 50 mL glass sampling bottles and the previously prepared perlite-particle samples No. 1, 5, and 6.

(2) Adjust the peristaltic pumps so that the three pumps operate at flow rates of 10, 20, and 30 mL/min, respectively. Because the mechanical speed differs from pump to pump, the flow rate of each pump should be calibrated according to its actual rotational speed. For example, when the pump speed is adjusted to 20 r/min, the flow discharged from the outlet within 1 min is

ISSN: 2688-8645

measured with an appropriate graduated cylinder. If the target flow rate is 10 mL/min, a 10 mL cylinder can be used to measure the 1 min discharge. If the measured flow does not meet the requirement, the pump speed is decreased or increased and the measurement is repeated until the required flow rate is reached.

Fig 4. Photograph of the experimental setup

(3) Fill the above three groups of particles into three plastic tubes, connect the rubber tubes and peristaltic pumps, and complete the assembly of the experimental apparatus.

(4) Fill the water reservoir with purified water, start the scouring test after all preparations are complete, and examine the effect of different scouring flow rates on sustained-release behavior.

(5) When purified water has completely submerged the scouring chamber and the outlet has been discharging for 1 min, collect a sample at the outlet using a 50 mL glass bottle and record it as the 0 h sample. Then collect samples every 1 h, for a total of seven times. After 7 h, collect one sample every 2 h. During the sampling period, make sure that there is sufficient purified water in the reservoir so that the scouring results are not affected.

3.2.2. Effect of Temperature on Sustained-Release Performance

(1) Prepare several 50 mL glass sampling bottles and particle samples No. 1, 4, and 9.

(2) Adjust the peristaltic pumps so that all three pumps operate at 10 mL/min.

(3) Fill the above three particle groups into three plastic tubes, connect the rubber tubes and peristaltic pumps, and place the inlet rubber tubes of the No. 4 and No. 9 test groups into water baths at 40°C and 60°C, respectively. The actual water-bath temperature should be slightly higher than the preset temperature. Then complete the assembly of the experimental apparatus.

(4) Fill the water reservoir with purified water, start the scouring test after all preparations are complete, and investigate the effect of temperature on sustained-release behavior.

(5) When purified water has completely submerged the scouring chamber and the outlet has been discharging for 1 min, collect the 0 h sample at the outlet using a 50 mL glass bottle. Then collect samples every 1 h, for a total of seven times. After 7 h, collect one sample every 2 h. During the sampling period, ensure that the reservoir contains enough purified water so that the experimental results are not affected.

3.2.3. Effect of Particle Size on Sustained-Release Performance

(1) Prepare several 50 mL glass sampling bottles and the previously prepared particle samples No. 1, 2, and 3.

(2) Adjust the three peristaltic pumps to 10 mL/min.

(3) Fill the above particle groups into three plastic tubes, connect the rubber tubes and peristaltic pumps, and complete the assembly of the experimental apparatus.

ISSN: 2688-8645

(4) Fill the reservoir with purified water, start the scouring experiment after all preparations are complete, and investigate the effect of different particle sizes on sustained-release performance.

(5) When purified water has completely submerged the scouring chamber and the outlet has been discharging for 1 min, collect the 0 h sample at the outlet using a 50 mL glass bottle. Then collect samples every 1 h, for a total of seven times. After 7 h, collect one sample every 2 h. During the sampling period, ensure that the reservoir contains enough purified water so that the experimental results are not affected.

3.2.4. Effect of Active-Component Content on Sustained-Release Performance

(1) Prepare several 50 mL glass sampling bottles and the prepared particle samples No. 1, 7, and 8.

(2) Adjust the three peristaltic pumps to 10 mL/min.

(3) Fill the above three groups of perlite particles into three plastic tubes, connect the rubber tubes and peristaltic pumps, and complete the assembly of the experimental apparatus.

(4) Fill the reservoir with purified water, start the scouring experiment after all preparations are complete, and investigate the sustained-release performance of particles with different active-component contents.

(5) When purified water has completely submerged the scouring chamber and the outlet has been discharging for 1 min, collect the 0 h sample at the outlet using a 50 mL glass bottle. Then collect samples every 1 h, for a total of seven times. After 7 h, collect one sample every 2 h. During the sampling period, ensure that the reservoir contains enough purified water so that the experimental results are not affected.

4. Results and Discussion

Based on the above experiments, the test data were sorted and processed in this section. The release performance of this natural-skeleton tracer particle under different constraints was obtained and interpreted accordingly.

4.1. Effect of Scouring Flow Rate on Sustained-Release Performance

To investigate the effect of scouring flow rate on the sustained-release performance of the natural-skeleton particles, the flow rate was varied while the other variables were kept constant: temperature = 20°C, particle size = 2-4 mm, and active-component content = 10%. The experimental results are shown in Figs. 5-7.

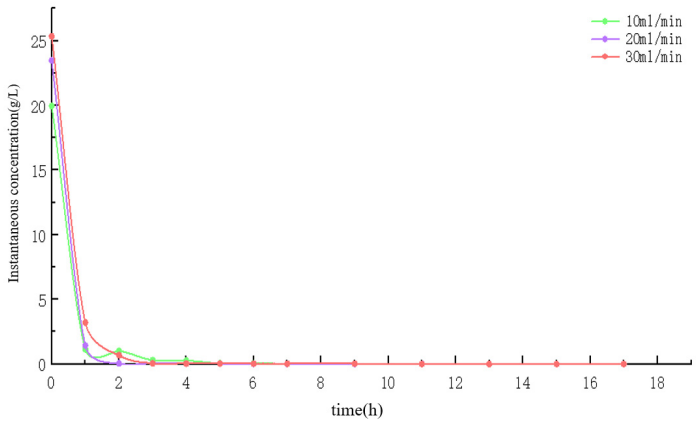

Fig 5. Instantaneous bromide-ion concentration at different scouring flow rates

ISSN: 2688-8645

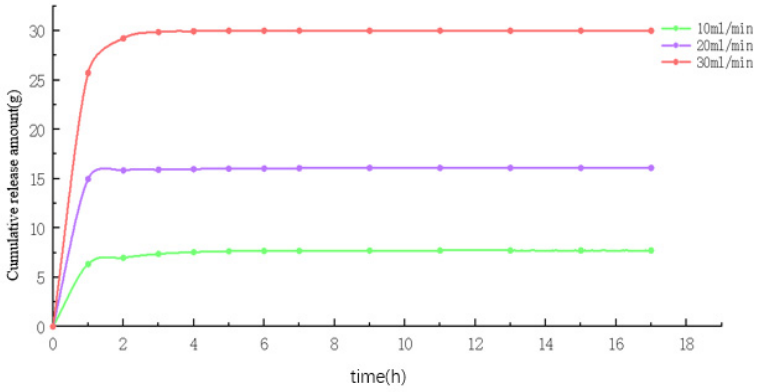

Fig 6. Cumulative bromide-ion release at different scouring flow rates

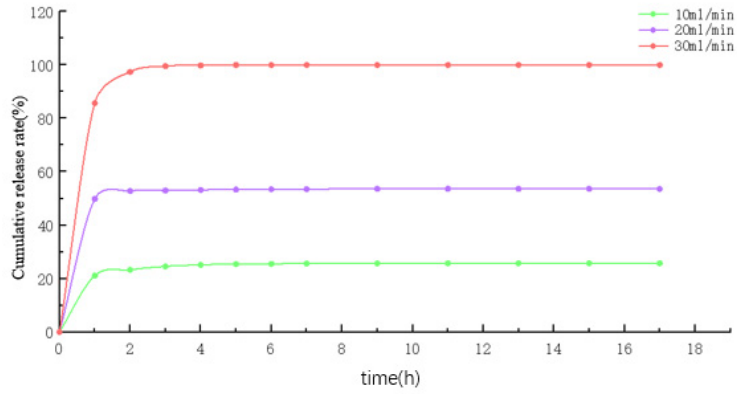

Fig 7. Cumulative bromide-ion release ratio at different scouring flow rates

Figure 5 shows that, as the experiment proceeded, the bromide-ion concentration under all flow-rate conditions generally decreased and eventually approached zero. The higher the flow rate, the higher the initial bromide-ion concentration and the slower the concentration decline. Combined with Figs. 6 and 7, it can be seen that a higher flow rate causes the perlite particles containing the same amount of reagent to release a larger amount of tracer, and this effect persists with time. The release ratio also increases with increasing flow rate. Under a flow rate of 30 mL/min, the reagent contained in the perlite particles was almost completely released. Figure 7 further indicates that under scouring rates of 10 and 20 mL/min, the active component in the perlite particles could not be fully released; after 17 h, the release ratios were only 25% and 53%, respectively, whereas the release at 30 mL/min was nearly complete. These results demonstrate that the intelligent tracer is highly sensitive to water-flow velocity and can clearly discriminate different flow conditions. The slight deviation in the data at 2 h may have been caused by nonstandard sampling operations or nonuniform adsorption during reagent loading.

4.2. Effect of Temperature on Sustained-Release Performance

To investigate the effect of temperature on the sustained-release performance of the natural-skeleton particles, the temperature was varied while the other variables were kept constant: scouring flow rate = 10 mL/min, particle size = 2-4 mm, and active-component content = 10%. The results are shown in Figs. 8-10.

ISSN: 2688-8645

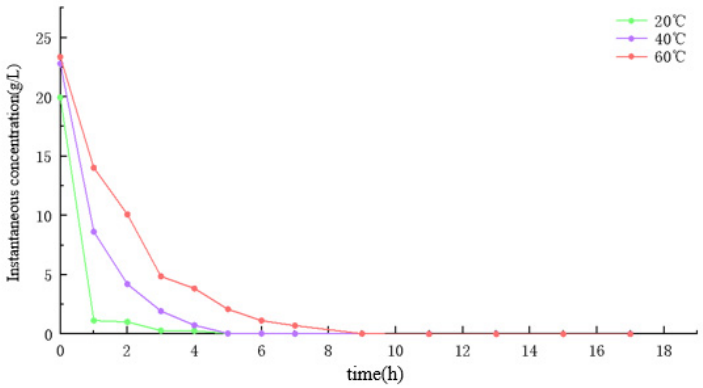

Fig 8. Instantaneous bromide-ion concentration at different temperatures

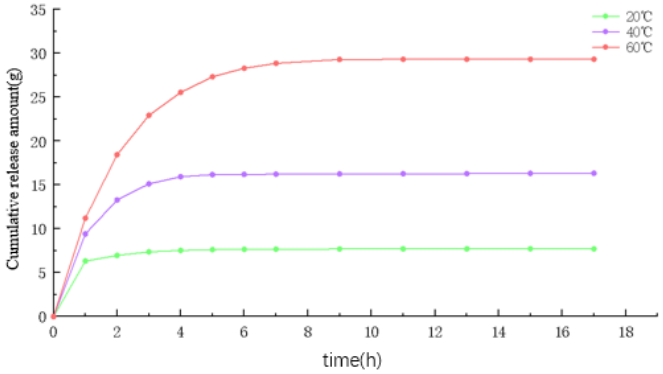

Fig 9. Cumulative bromide-ion release at different temperatures

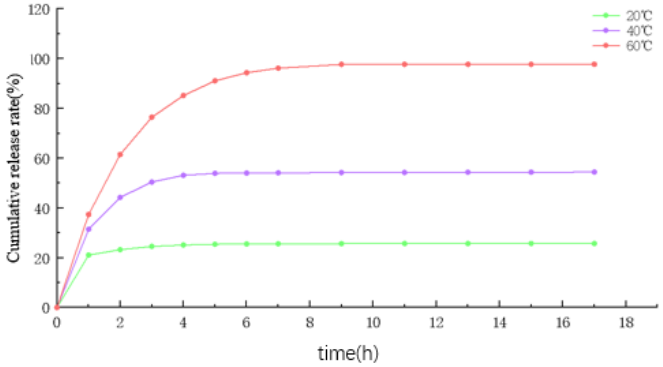

Fig 10. Cumulative bromide-ion release ratio at different temperatures

Figure 8 shows that the bromide-ion concentration generally decreased with time under different temperature conditions, which is similar to the trend observed for the flow-rate experiments. However, the effect of temperature on concentration decline was more obvious than the difference caused by changing flow rate within the same period. The higher the temperature, the higher the initial released bromide-ion concentration, and because the cumulative release kept increasing, the concentration declined more slowly. Combined with Figs. 9 and 10, it can be seen that within the first hour the effect of temperature on the bromide-

ISSN: 2688-8645

ion release rate was relatively small, but as the experiment continued, higher temperature caused perlite particles containing the same amount of reagent to release more tracer. The longer the time, the more pronounced the effect. The release ratio also increased with increasing temperature. At 60°C and 10 mL/min, the reagent contained in the perlite particles was almost completely released under the present test conditions.

4.3. Effect of Particle Size on Sustained-Release Performance

To investigate the effect of particle size on the sustained-release performance of the natural-skeleton particles, the particle size was varied while the other variables were kept constant. The experimental results are shown in Figs. 11-13.

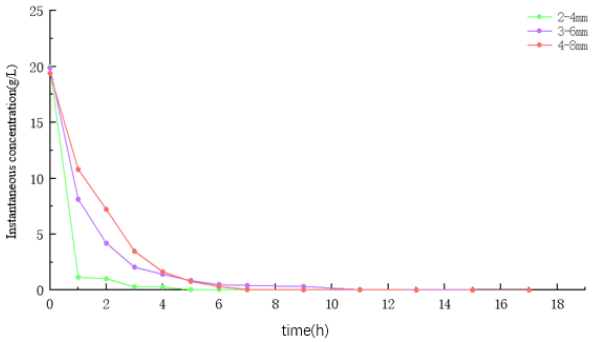

Fig 11. Instantaneous bromide-ion concentration at different particle sizes

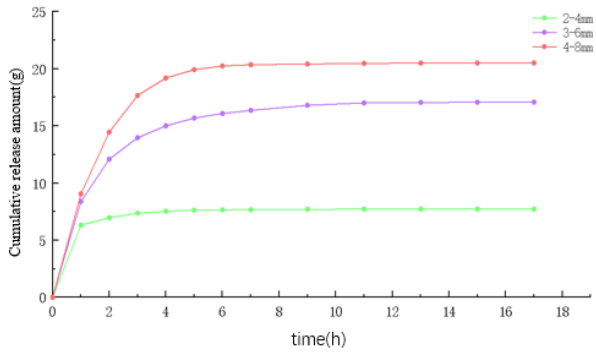

Fig 12. Cumulative bromide-ion release at different particle sizes

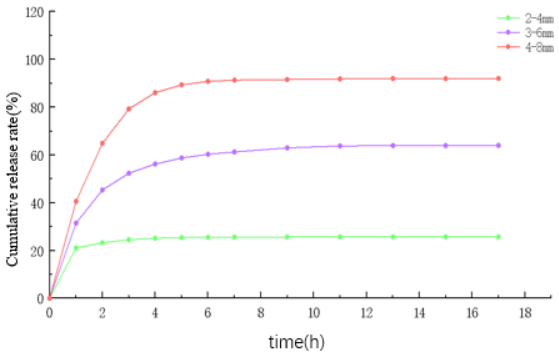

Fig 13. Cumulative bromide-ion release ratio at different particle sizes

ISSN: 2688-8645

Figure 11 shows that the release concentration of perlite particles with different particle sizes differed, as did the rate of change. Overall, with increasing particle size, the release concentration became higher and the concentration changed more slowly. Under the same scouring flow rate, temperature, and reagent content, larger perlite particles were more likely to achieve complete release. Combined with Figs. 12 and 13, it can be seen that larger perlite particles released a greater cumulative amount of reagent. In particular, the cumulative release from 4-8 mm particles differed significantly from that of the other two particle-size groups (2-4 mm and 3-6 mm), and the cumulative release ratio also showed a marked difference.

4.4. Effect of Active-Component Content on Sustained-Release Performance

To investigate the effect of active-component content on the sustained-release performance of the natural-skeleton particles, the particles were impregnated with sodium bromide solutions of different concentrations while the other variables—temperature, scouring flow rate, and particle size—were kept constant. The results are shown in Figs. 14-16.

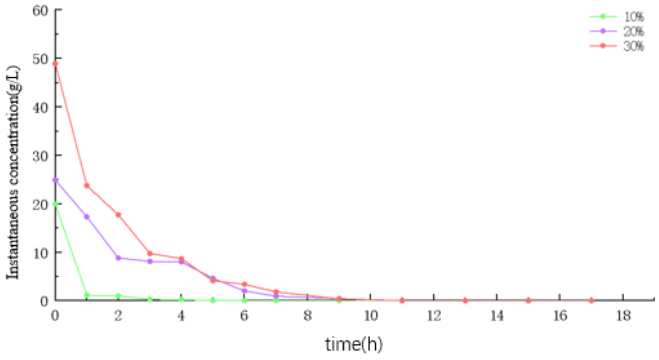

Fig 14. Instantaneous bromide-ion concentration at different active-component contents

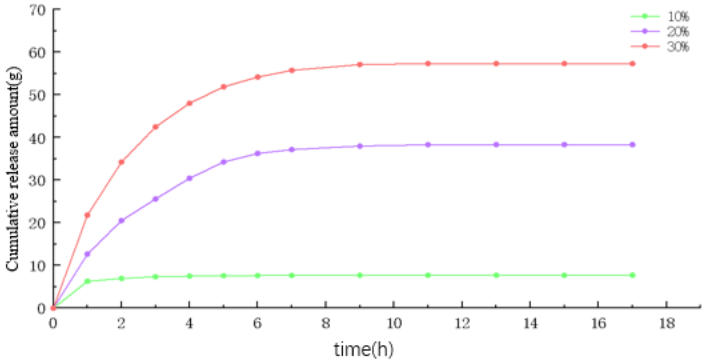

Fig 15. Cumulative bromide-ion release at different active-component contents

Figure 14 shows that the release concentration of perlite particles containing different mass fractions of sodium bromide differed greatly. Because the particles adsorbed sodium bromide solutions with different mass fractions, the particles loaded with the highest content, namely the 30 wt.% group, exhibited a much higher release concentration than the 20 wt.% and 10 wt.% groups. The trend in concentration change was generally similar to that observed in the previous three sets of experiments. Particles adsorbing more reagent were less likely to be completely released. Combined with Figs. 15 and 16, it can be seen that the greater the amount of adsorbed reagent, the greater the cumulative amount of released reagent. In comparison with the 30 wt.% group, the 10 wt.% and 20 wt.% groups showed large differences in both

ISSN: 2688-8645

cumulative release and cumulative release ratio. This factor also exhibited a relatively strong influence when compared with the other three factors.

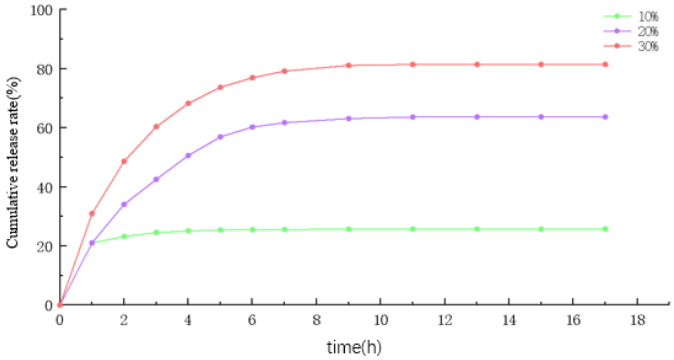

Fig 16. Cumulative bromide-ion release ratio at different active-component contents

5. Conclusion

(1) Through literature review and repeated experiments, the active component of the optimized natural-skeleton tracer was identified as perlite particles adsorbing sodium bromide.

(2) Scouring experiments and particle-characterization data for sodium-bromide-loaded natural-skeleton sustained-release tracer particles show that a faster scouring flow rate leads to a greater release of the active component; increasing temperature also increases the released amount; larger particles release the active component more easily; and a higher loaded reagent mass results in a greater amount of released active component.

(3) When other objective conditions are kept unchanged, scouring flow rate largely determines both the amount and rate of release. Tracer content, temperature, and particle size also affect the release of the active component from sustained-release tracer particles, but their influence is relatively smaller than that of scouring flow rate.

(4) The four objective factors—scouring flow rate, temperature, particle size, and active-component content—jointly determine whether the particles can be completely released within a certain period of time.

References

[1] Li Dajian, Zhu Hongzheng, Ma Guowei, et al. Current status of water-detection technologies for horizontal wells and discussion of rapid water-detection methods[J]. Petroleum Geology & Engineering, 2021, 35(1): 109-112, 117.

[2] Liao Maolin, Lei Zhanxiang, Zhao Hui, et al. Evaluation of waterflooding development effect in reservoirs with strong edge and bottom water[J]. Science Technology and Engineering, 2017, 17(27): 178-183.

[3] Zhang Tianlong, Wu Changhui, Liang Weiwei, et al. Water-cut characteristics of horizontal wells in tight oil reservoirs and influencing factors[J]. Petrochemical Industry Application, 2021, 40(1): 56-62.

[4] Ren Guohui, Zhao Xindi, Lu Yinghui, et al. Integrated geological-engineering technology for shale-gas perforation in southern Sichuan[J]. Well Logging Technology, 2021, 45(1): 87-92.

[5] Guo Xiao, Di Dejia, He Zuqing, et al. Interpretation method of production profiles using sustained-release quantum-dot tracers[J]. Science Technology and Engineering, 2022, 22(13): 5222-5227.

[6] Mayerhofer M J, Cipolla C L, Warpinski N R, et al. What is stimulated rock volume?[J]. SPE 119890, 2008.

[7] Li Zhiping, Wan Yiwen, Zhang Xiting. A new method for productivity evaluation of gas wells in low-permeability gas reservoirs[J]. Natural Gas Industry, 2007(4): 85-87, 156-157.

[8] Wei Yunsheng, Jia Ailin, He Dongbo, et al. A new idea for productivity evaluation of staged-fractured horizontal wells in tight-gas reservoirs[J]. Drilling & Production Technology, 2012, 35(1): 32-34, 9.

[9] Wang Daiguo, Kong Fanzheng. Analysis of factors affecting gas-layer productivity in the Permian reservoir of the Hangjinqi block[J]. Journal of Chang'an University (Earth Science Edition), 2003(3): 38-40, 47.

[10] Mayerhofer M J, Lolon E P, Youngblood J E, et al. Integration of microseismic fracture mapping results with numerical fracture-network production modeling in the Barnett Shale[R]. SPE 102103, 2006.

[11] Li Huayang, Deng Jingen, Feng Yongcun, et al. Research status and development trend of oilfield tracer technology[J]. Applied Chemical Industry, 2023, 52(11): 3163-3168, 3174.

[12] Yuan Qing, Bi Yanxia, Li Fengguang, et al. Progress in the application of sustained-release technology in oilfields[J]. Petrochemical Industry Application, 2016, 35(1): 1-4.

[13] Li Yan, Duan Yonggang, Wei Mingqiang. Research on the application of sustained-release technology in oil and gas field development[C]// Chinese Society of Theoretical and Applied Mechanics. Proceedings of the Chinese Congress of Theoretical and Applied Mechanics 2021+1 (Vol. 3). School of Petroleum and Natural Gas Engineering, Southwest Petroleum University, 2022: 1.